Toward elucidating the mechanism of femtosecond pulse shaping control in photodynamics of molecules by velocity map photoelectron and ion imaging

Daniel Irimia and Maurice H. M. Janssen

Citation: J. Chem. Phys. **132**, 234302 (2010); doi: 10.1063/1.3436720
View online: http://dx.doi.org/10.1063/1.3436720
View Table of Contents: http://jcp.aip.org/resource/1/JCPSA6/v132/i23
Published by the American Institute of Physics.

Toward elucidating the mechanism of femtosecond pulse shaping control in photodynamics of molecules by velocity map photoelectron and ion imaging

Daniel Irimia and Maurice H. M. Janssen[a)]
Department of Chemistry and Laser Centre, Vrije Universiteit, de Boelelaan 1083, 1081 HV Amsterdam, The Netherlands

(Received 16 March 2010; accepted 5 May 2010; published online 15 June 2010)

The control of photofragmentation and ionization in a polyatomic molecule has been studied by femtosecond chirped laser pulse excitation and velocity map photoelectron and ion imaging. The experiments aimed at controlling and investigating the photodynamics in CH_2BrCl using tunable chirped femtosecond pulses in the visible wavelength region 509–540 nm at maximum intensities of about 4×10^{13} W/cm^2. We observe that the time-of-flight mass spectra as well as the photoelectron images can be strongly modified by manipulating the chirp parameter of ultrashort laser pulses. Specifically, a strong enhancement of the CH_2Cl^+/CH_2BrCl^+ ion ratio by a factor of five and changes in the photoelectron spectra are observed for positively chirped pulses centered near 520 nm. These changes are only observed within a narrow window of wavelengths around 520 nm and only for positively chirped pulses. From the combination of the photoelectron spectra and the ion recoil energy of the CH_2Cl^+ fragment we can deduce that the parent ionization and fragmentation is induced by a multiphoton excitation with five photons. The photoelectron images and the fragment ion images also provide the anisotropy (β-parameter) of the various electron bands and fragment ions. We conclude that multiphoton excitation of the highest occupied 22a′ and 8a″ CH_2BrCl molecular orbitals of Br-character are both involved in the five-photon ionization, however, only excitation of the 22a′ orbital appears to be (mostly) involved in the chirped control dynamics leading to enhanced fragmentation to $CH_2Cl^+(\tilde{X}\ A')+Br(^2P_{3/2})$. We propose that a wavepacket following or a time-delay resonance mechanism between the two-photon excited $n_x(Br,22a')\rightarrow(2A')$ repulsive surface and the three-photon near-resonant $n_x(Br,22a')\rightarrow$Rydberg(A′) state of the neutral CH_2BrCl molecule is responsible for the enhanced excitation of the $n_x(Br,22a')$ molecular orbital with up-chirped pulses. This leads to enhanced ionization to a configuration in the $CH_2BrCl^+(\tilde{X}\ A')$ continuum just above the dissociation limit of the $CH_2Cl^+ + Br(^2P_{3/2})$ channel, resulting in enhanced fragmentation. © *2010 American Institute of Physics*.
[doi:10.1063/1.3436720]

I. INTRODUCTION

One of the goals of molecular reaction dynamics is to understand in full detail the processes leading to the breaking and formation of a chemical bond. Of particular interest is the partitioning of energy within the reaction products and how to maximize the yield of desired products and to suppress the unwanted by-products. During the last decade the technique of coherent or optimal control has become a proliferating technique for the study of selective molecular dissociation and ionization, chemical reactions and the control of molecular wavepacket dynamics.[1,2] The control of laser-matter interaction processes is accomplished by controlling the temporal and spectral shape of the interacting light pulses in such a way as to drive the outcome of a chemical process into the preferred direction. At present, one of the most popular control techniques is adaptive femtosecond pulse shaping[3] and for a recent overview of this rapidly growing field see, e.g., the special issues of Refs. 4–6 and references therein. The application of adaptive pulse shaping to study ionization and fragmentation dynamics in polyatomic molecules has been pioneered by the experimental groups of Gerber[7] and Levis.[8] The interpretation of some of the experimental observations appears to be open to intense scientific debate[9,10] and some more general conclusions regarding the (lack of) coherence in the control of molecular (ionic) fragmentation in larger polyatomic molecules were proposed recently by Dantus and co-workers.[11] Until now most experimental studies using adaptive pulse shaping on polyatomic molecules have used time-of-flight (TOF) mass spectrometric detection. This technique provides only information on the masses of the various ionic fragments produced and very limited information on the mechanism of the dynamics involved. In some cases extensive theoretical wavepacket calculations on reduced dimensionality potential energy surfaces have been used to interpret results of polyatomic adaptive control experiments.[12]

The introduction of multidimensional particle imaging techniques in chemical dynamics[13] has enabled researchers

a)Author to whom correspondence should be addressed. Electronic mail: mhmj@chem.vu.nl.

to reveal molecular dynamics at unprecedented detail.[14–23] Especially, the combination of photoelectron-photoion coincidence imaging with femtosecond time-resolved spectroscopy has been shown to provide extremely insightful information on multiphoton multichannel dynamics.[24–27]

In this paper, we report our first results combining velocity map (noncoincidence) electron and ion imaging techniques with ultrafast pulse shaping to study the control of molecular ionization and fragmentation processes in polyatomic molecules. We have chosen a relatively small molecule, CH_2BrCl, as a target system to make (future) comparison with theoretical calculations more tractable. The photochemistry of halocarbons received a lot of attention during the last decades arising from the fact that they contribute significantly to atmospheric changes, especially to the destruction of ozone in the Earth's stratosphere. The halocarbons have a long lifetime at low altitudes due to high resistance to biodegradation and photochemical fragmentation; however, in the higher atmosphere the UV solar radiation is very efficient in bondbreaking leading to the formation of halogen-containing radicals and halogen atoms. After the absorption of UV photons, CH_2XY molecules are excited to various dissociative states where an electron is promoted from a lone pair orbital of the halogen atom to a carbon-halogen antibonding molecular orbital giving rise to a free halogen atom and halomethyl radicals CH_2X. These radicals can still absorb more photons releasing the second halogen atom. Halomethanes such as CH_2BrCl have different electronic symmetries (because of the symmetry lowering due to the different halogens), more complex UV absorption spectra and a greater number of dissociation channels (pathways) involved in photofragmentation compared with monohalogen molecules such as CH_2Br_2.

CH_2BrCl has been studied before by Gerber and co-workers[28] in adaptive pulse shaping experiments at 800 nm using TOF mass detection. In those experiments, the goal was to find specific phase-shaped pulses to affect the molecular dynamics in such a way as to maximize the formation of ionic fragments where the strongest bond is broken, i.e., to maximize the ratio of CH_2Br^+/CH_2Cl^+. The experimental observation at 800 nm was an increase of the fission of the stronger versus the weaker carbon halogen bond, i.e., an increase of the CH_2Br^+/CH_2Cl^+ ratio by about 80%, using an adaptively shaped pulse. However, no interpretation of the mechanism was presented in the study by Gerber and co-workers.[28]

The photodynamics of the halomethane system have also been studied in the past using chirped femtosecond pulse shaping. The chirp is well recognized as a weighty parameter that can be used to manipulate the dynamics of a system interacting with ultrafast laser pulses.[29] The chirp, known also as a frequency sweep, characterizes the laser pulse besides intensity, duration and frequency and is for instance produced by the propagation of the laser pulses through dispersive materials. A pioneering study on the enhancement of multiphoton absorption in I_2 using chirped pulses around 600 nm was reported by Wilson and co-workers.[30] Femtosecond pulse chirping was applied by Dantus and co-workers[31] to control the photodissociation reaction of CH_2I_2 monitoring the concerted release of the I_2 molecule by fluorescence. More recently, the group of Weinacht has reported several studies using pump-probe spectroscopy to study wavepacket dynamics and control in halomethanes.[32–34] From these multiphoton excitation studies at 800 nm, Weinacht and coworkers conclude that resonances between ionic surfaces of the parent ion facilitate the formation of ionic fragments.

In this paper we examine the photodynamics of CH_2BrCl using ultrafast chirped laser pulses in conjunction with (noncoincidence) photoelectron and photoion velocity map imaging detection. We performed experiments with femtosecond laser pulses centered at 509, 521, and 540 nm. At all three wavelengths there are only two major ionic products observed, the CH_2BrCl^+ parent ion and the CH_2Cl^+ fragment ion, corresponding to the loss of a bromine atom. In our experiments we find that only excitation at 521 nm is able to control the fragmentation ratio significantly with up-chirped pulses, and the selectivity is achieved within a very narrow spectral window only. In Sec. II, we present our experimental setup and in Sec. III we present our data. We discuss the present results in Sec. IV and summarize our conclusions in Sec. V.

II. EXPERIMENTAL

The molecular beam machine and imaging detector that are used in the present experiments have been described previously.[35–38] In brief terms, the molecular beam was prepared by seeding 5% CH_2BrCl in He which expands through a pulsed (1 kHz) homebuilt piezovalve with a 300 μm nozzle. The molecular beam is doubly skimmed and crossed by femtosecond laser pulses about 150 mm downstream from the nozzle orifice. The typical backing pressure behind the nozzle is 1 bar. We noticed during the course of the experiments that high seeding ratios or pure beams of CH_2BrCl easily resulted in (large) cluster and droplet formation hampering the proper operation of our pulsed piezovalve. Therefore, in all experiments reported here fractions of 5% (or less) CH_2BrCl were used. The interaction of the femtosecond pulses with CH_2BrCl leads to various photodynamical events and the released photoproducts are monitored using either TOF mass-gated ion detection followed by velocity map ion imaging (with a charge-coupled-device camera) or TOF electron detection followed by velocity map electron imaging. The detection of either ions or electrons was set by choosing the proper voltages on the velocity map ion lenses. The micro-channel-plate detector was gated using homebuilt fast (about 5 ns) or variable duration high-voltage pulsers.[39]

The tunable chirped femtosecond laser pulses are produced by a homebuilt two-stage noncollinearly phase-matched optical parametric amplifier (NOPA).[40,41] The NOPA is seeded by a white light continuum produced by focusing 800 nm pulses (about 120–150 fs) of a Ti:sapphire regenerative amplifier (Spectra Physics Spitfire) in a sapphire plate. The two parametric amplifying BBO (beta-BaB_2O_4) crystals in the NOPA are pumped by the frequency-doubled

blue light near 400 nm. The homebuilt NOPA can be continuously tuned through the visible spectral region (500–700 nm), though for our present study only a wavelength range from 509 to 540 nm was used. NOPA output pulses are compressed in a double pass prism compressor and the linear chirp is varied by inserting more or less prism material (N-SSK8) in the beam path. The shortest visible NOPA pulses after the compressor have widths of typically about 25–35 fs for all used wavelengths (509–540 nm) and the output energies obtained are about 20 μJ. For temporal characterization of the NOPA pulses we employed second harmonic autocorrelation in a 75 μm BBO crystal.[42] The spectrum of the NOPA pulses was measured with an Ocean Optics spectrometer. After compression the pulse energy measured before the entrance window of the ionization chamber in the molecular beam machine is around 15 μJ. The NOPA pulses pass through several dispersive elements, such as a focusing lens and an input window, from the exit of the compressor to the interaction point in the molecular beam. To measure as carefully as possible the real duration of the pulses as they are when interacting with the molecular beam we maximized the collinear second harmonic generation in a BBO crystal located near the setup. This provided the best calibration of the position of the prism compressor for bandwidth limited pulses in the interaction region. We estimate that for the shortest duration pulses with the focusing lens used (focal length 40 cm) the peak intensity in the molecular beam interaction region is about 4×10^{13} W/cm^2.

The amount of chirp in the pulse was changed by changing the amount of prism material which was carefully measured. The resulting chirp was calculated using the material properties of the compressor and by comparison with the measured pulse duration in an intensity autocorrelator. The measured autocorrelation of the chirped pulses was in accordance with the calculated chirp.

III. RESULTS

In Fig. 1, the TOF-spectra are shown as measured after multiphoton excitation using femtosecond laser pulses centered at 509, 521, and 540 nm. The laser pulses coming out of the prism compressor were optimized to be as short as possible (about 25–35 fs) and near transform-limited. At all three wavelengths the TOF-spectra exhibit two main peaks corresponding to the CH_2BrCl^+ parent ion and CH_2Cl^+ fragment ion. The TOF-spectra were measured under similar detection conditions, and the ion signals were scaled with respect to the intensity of the CH_2BrCl^+ ion peak recorded at 540 nm. We notice a change in the absolute ion yields, and a somewhat larger total ion yield is observed at 540 nm. Furthermore, we notice a change in the relative CH_2Cl^+/CH_2BrCl^+ ion ratio with central wavelength. The CH_2Cl^+ fragment ion dominates the TOF-spectrum at 509 nm, whereas the CH_2BrCl^+ parent is the largest ion peak at 540 nm. At 521 nm, both the parent ion and the CH_2Cl^+ fragment ion have very similar TOF intensities.

In Fig. 2, top panel (a) the absolute yield of CH_2BrCl^+ parent ions and CH_2Cl^+ fragment ions is shown as a function of linear chirp, for a pulse centered at 521 nm. In the bottom

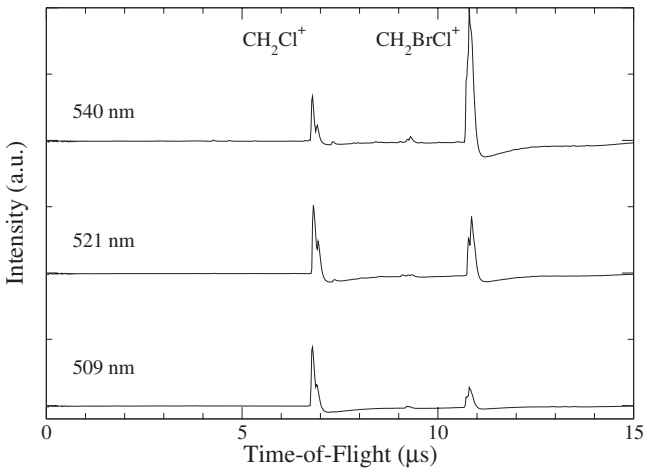

FIG. 1. TOF spectra of ions produced in the multiphoton femtosecond ionization of CH_2BrCl. The femtosecond laser pulses were as short as possible in duration (25–35 fs typically) with center wavelength at 540 nm (top), 521 nm (middle), and 509 nm (bottom). The spectral bandwidth of the pulses (FWHM) is about 20–27 nm. The dominant ions at all three wavelengths are CH_2BrCl^+ parent ions and CH_2Cl^+ fragment ions, with barely visible CH_2Br^+ fragment ions. A strong change with wavelength is seen for the relative yield of parent vs fragment ions.

panel (b) the ratio CH_2Cl^+/CH_2BrCl^+, as obtained from the top panel, is plotted as a function of linear chirp. The intensities of the two ions were measured under the same detection conditions so the absolute ion intensities can be compared to each other at the various chirp settings. We observe that the total absolute ion intensities exhibit their maximum at about 850 fs^2. It can be seen that the ion ratio $R=CH_2Cl^+/CH_2BrCl^+$ can be selectively controlled by variation of the pulse chirp. The ion ratio R shows an enhancement by about a factor of 5 when changing the chirp from down-chirp (−560 fs^2) to up-chirp (1700 fs^2). A minimum $R\approx0.5$ is observed for negative chirp near −560 fs^2 and a maximum ratio $R\approx2.3$ is obtained near 1700 fs^2 positive chirp. This chirp variation corresponds to a change in temporal width extending from about 55 fs (when −560 fs^2 linear chirp) to about 200 fs (when 1700 fs^2).

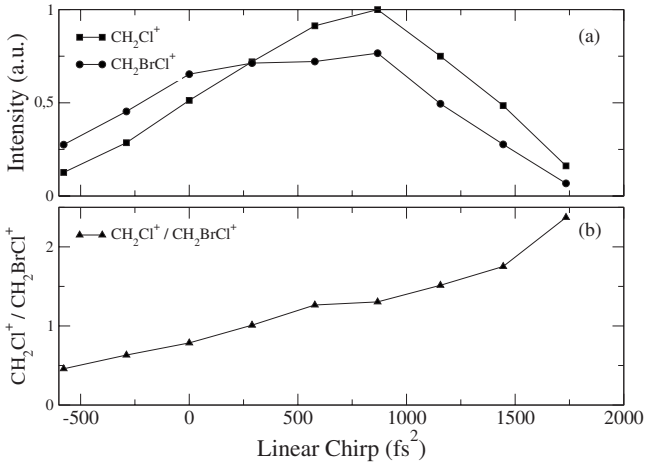

FIG. 2. In the top panel (a) the absolute yield of CH_2BrCl^+ parent ions and CH_2Cl^+ fragment ions is shown as a function of linear chirp, for a pulse centered at 521 nm. In the bottom panel (b) the ratio CH_2Cl^+/CH_2BrCl^+, as obtained from the top panel, is plotted as a function of linear chirp.

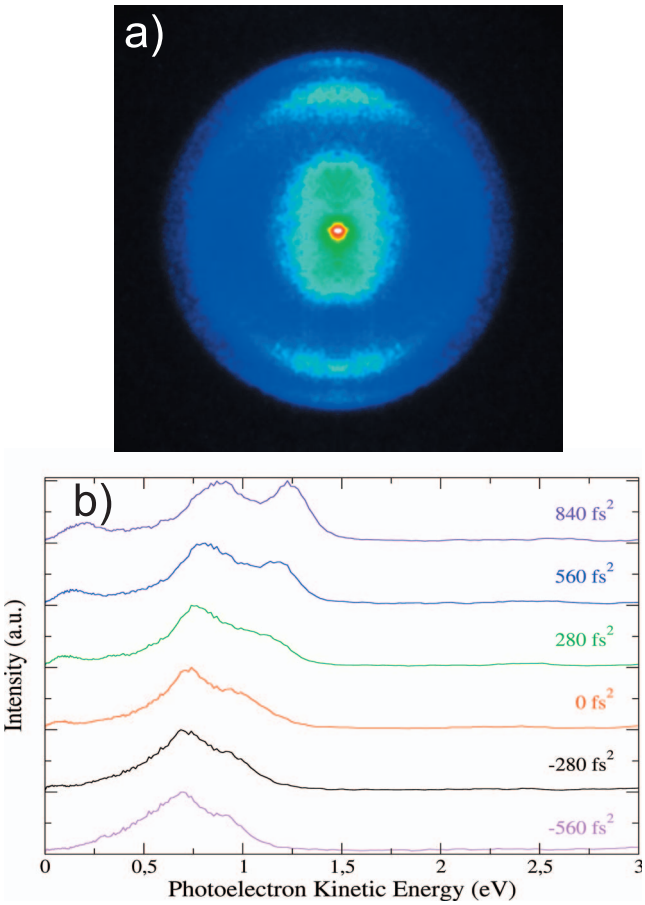

FIG. 3. In the top panel (a) the photoelectron raw data image as obtained for an up-chirped pulse of +840 fs^2 centered at 521 nm is shown. In the bottom panel (b) the photoelectron spectra obtained from the Abel-inverted photoelectron raw images for femtosecond pulses centered at 521 nm are shown for varying linear chirp.

The photoelectron spectra of CH_2BrCl at 521 nm for different chirped pulse excitation, as obtained from the photoelectron images, are shown in Fig. 3. We observe that near zero and at negative chirp values, the electron distribution is dominated by a somewhat broadened peak at 0.7–0.9 eV. At positive chirp three more clearly separated peaks appear in the spectrum with energies at about 0.15, 0.9, and 1.2 eV.

The chirped laser experiments were also done at other wavelengths, 509 nm and 540 nm, but the chirp dependency on the ion fragmentation was not as significant as observed at 521 nm. In Fig. 4, the photoelectron spectra are shown as obtained from photoionization of CH_2BrCl with down-chirped (−320 fs^2), unchirped (0 fs^2) and up-chirped (+320 fs^2) laser pulses centered at 540 nm, and in Fig. 5 for pulses centered at 509 nm and down-chirped (−450 fs^2), unchirped (0 fs^2) and up-chirped (+450 fs^2). We observe relatively small changes with chirp in the photoelectron spectra and did not see the clear changes in the mass ratio CH_2Cl^+/CH_2BrCl^+ with chirp for pulses centered at wavelengths near 540 or 509 nm. Therefore, we will focus the discussion of our results in this paper on the experimental results obtained at 521 nm.

Finally, in Fig. 6 we present the kinetic energy distributions of the $CH_2Cl^+ + Br$ channel obtained from velocity map images of the CH_2Cl^+ ions recorded with negative and positive chirped laser pulses centered at 521 nm. In both spectra we distinguish a dominant peak with total kinetic energy at low values around 0.08 eV and a cutoff kinetic energy of about 0.4 eV. As the linear chirp changes from negative to positive there seems to be just a slight shift of the kinetic energy to higher values.

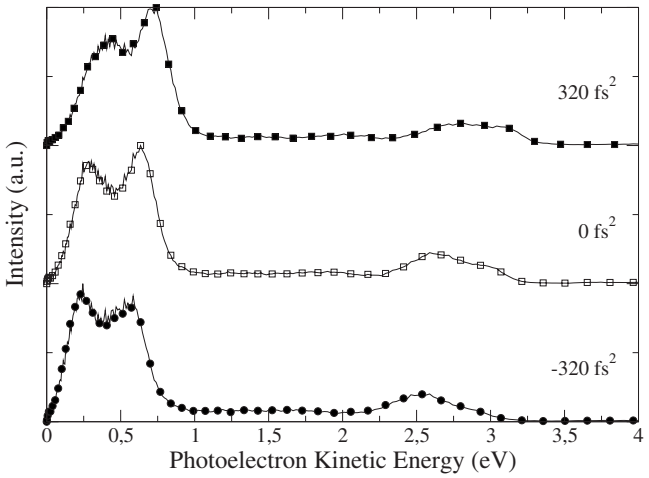

FIG. 4. Photoelectron spectra obtained from the photoelectron images for femtosecond pulses centered at 540 nm and varying linear chirp.

IV. DISCUSSION

A. Multiphoton excitation and photoelectron spectra

In Fig. 7, we show the location of the lowest energy levels in the CH_2BrCl^+ parent ion and the $CH_2Cl^+ + Br(^2P_{3/2}, ^2P_{1/2})$ fragmentation channels. Photoelectron spectroscopy experiments[43] reveal that just above threshold there are four photoelectron bands related to the CH_2BrCl^+ cation and they were observed at 10.75, 11.08, and 11.79 eV (unresolved structure). The first two bands at 10.75 and 11.08 eV correspond to ionization of the bromine lone-pair electron and the level is split as a result of the strong spin-orbit coupling in CH_2BrCl^+ due to the Br atom. The third and fourth bands were unresolved and have the character of ionization of the chlorine lone-pair orbital. More recently,

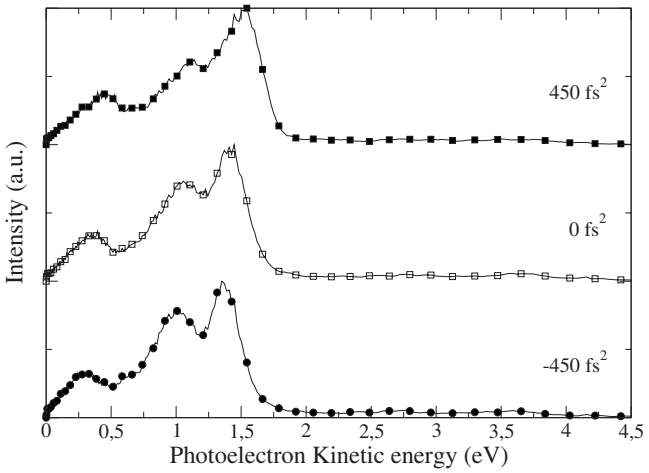

FIG. 5. Photoelectron spectra obtained from the photoelectron images for femtosecond pulses centered at 509 nm and varying linear chirp.

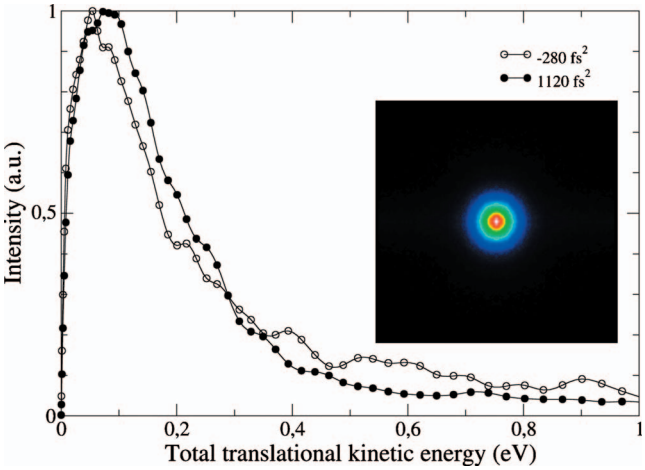

FIG. 6. Total kinetic energy released into the $CH_2Cl^+ + Br$ channel for femtosecond pulses centered at 521 nm with different linear chirp.

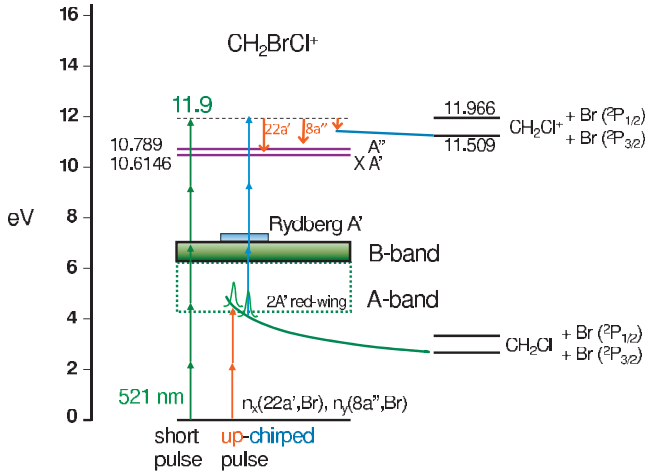

FIG. 7. Location of the relevant energy levels of the parent ion CH_2BrCl^+ and the $CH_2Cl^+ + Br$ channels. On the left side, we indicate the total energy of five-photon excitation with femtosecond pulses centered at 521 nm. On the right side we show the schematic of the proposed mechanism of wave-packet following or time-delay resonance at the two-to-three photon transition between the two-photon excited repulsive $(2A')$ red-wing of the A-band and the A' Rydberg level at three-photon excitation. The up-chirped pulses will enhance the excitation of the $n_x(Br,22a')$ orbital in the five-photon excitation resulting in an enhanced ejection of a low (0.1–0.2 eV) energy photoelectron and fragmentation to $CH_2Cl^+ + Br(^2P_{3/2})$.

pulsed field ionization-photoelectron experiments by Ng and co-workers[44] have provided the most accurate value of the lowest energy level of the parent ion $CH_2BrCl^+(\tilde{X}\ A')$, IE=10.6146 eV. The lowest ionic dissociation channel is $CH_2Cl^+ + Br(^2P_{3/2})$ and the appearance energy (AE) of this channel was also carefully determined, AE=11.509 eV. Furthermore, using calculations Ng and co-workers[44] also assigned the location of the lowest electronically excited ionic state $CH_2BrCl^+(\tilde{A}\ A'')$ as 0.174 eV above the ground state, i.e., at 10.789 eV. The location of these levels in the parent molecule and the lowest two dissociation channels, $CH_2Cl^+ + Br(^2P_{3/2}, ^2P_{1/2})$ are indicated in Fig. 7. The reason that the experimental photoelectron values of Tian *et al.*[43] are somewhat higher than the more recent values as obtained by Ng and co-workers[44] is that there is a rather large difference of about 22° in the Br–C–Cl equilibrium bending angle between the neutral CH_2BrCl ground state and the ionic $CH_2BrCl^+(\tilde{X}\ A')$ ground state, i.e., poor Franck–Condon overlap resulting in vibrationally excited ion levels in photoionization.

Multiphoton excitation with five photons at 521 nm (each photon is 2.38 eV with an energy full width at half maximum (FWHM)-bandwidth of about 0.105 eV) provides a total energy of 11.9 eV which is 1.29 eV above the lowest energy level of the CH_2BrCl^+ parent ion, and just 0.4 eV above the location of the $CH_2Cl^+ + Br(^2P_{3/2})$ fragmentation channel. Six photons at 521 nm provide a total excitation of 14.3 eV, which is far above the AE of the $CH_2Cl^+ + Br$ fragmentation channel.

To assign the peaks in the photoelectron spectra of CH_2BrCl (see Figs. 3–5), we reason as follows. From the TOF spectrum of CH_2BrCl at 540 nm (Fig. 1) we notice that the parent ion is mostly produced at 540 nm (2.30 eV per photon). The photoelectron spectrum at 540 nm (Fig. 4) and no chirp contains two dominant photoelectron peaks near 0.25 and 0.65 eV, separated by about 0.4 eV. These peaks we assign to a five photon ionization process with a total excitation energy of 11.5 eV and the formation of $CH_2BrCl^+(\tilde{X}\ A')$ ground state and electronically excited $CH_2BrCl^+(\tilde{A}\ A'')$ parent ion. Tian *et al.*[43] observed these similar two electron peaks separated by about 0.33 eV. This total excitation energy is also very close to the fragmentation threshold of 11.509 eV of $CH_2Cl^+ + Br(^2P_{3/2})$, so we do not think that direct five-photon excitation produces much fragmentation, as we should see a near 0 eV photoelectron peak. However, absorption of a sixth photon by the parent brings the system well above this threshold. That such a six-photon absorption also happens can be seen in Fig. 4 where there are quite pronounced photoelectron peaks around 2.5–2.8 eV, i.e., shifted by one photon of 2.30 eV (540 nm).

When we increase the photon energy from 2.30 eV (540 nm) to 2.38 eV (521 nm) to 2.44 eV (509 nm), we see that these two photoelectron peaks shift in energy with about five times the energy difference. E.g., at 509 nm we observe the two peaks near 1.1 and 1.4 eV, i.e., shifted by $(1.1-0.25)/5=0.17$ eV, or $(1.4-0.65)/5=0.15$ eV, close to the energy difference of 0.14 eV between the 509 nm (2.44 eV) and 540 nm (2.30 eV) photons.

For excitation at 521 nm and 509 nm we observe a third peak at lower photoelectron energy, near 0.1 eV for 521 nm excitation (Fig. 3) and near 0.35 eV for 509 nm excitation (Fig. 5). We assign this peak to a five-photon excitation followed by fragmentation to $CH_2Cl^+ + Br(^2P_{3/2})$. The total excitation energy is 11.9 eV (521 nm) or 12.18 eV (509 nm) and if we subtract the photoelectron energy at these two excitation wavelengths we obtain an available energy of 11.8 eV. From the ion image of Fig. 6 at 521 nm excitation we see that the total kinetic energy of the $CH_2Cl^+ + Br$ channel is about 0.1 eV. This leaves only little energy of about $11.8-0.1-11.509=0.19$ eV for internal excitation of the CH_2Cl^+ fragment.

It is interesting to note that especially near 521 nm when we change the chirp from down-chirp to up-chirp (Fig. 3) the intensity of this small peak near 0.1 eV increases in intensity

relative to the most intense peak near 0.8 eV. As we noticed in the mass spectra, when changing the chirp from down-chirp to up-chirp (Fig. 2), we clearly enhance the fragmentation to CH_2Cl^+ and this correlates with an increase of the photoelectron peak near 0.1 eV as assigned to the $CH_2Cl^+ + Br$ channel.

A last remark at this moment while discussing the photoelectron spectra is that for all three photoelectron spectra (Figs. 3–5), it appears that the second of the two peaks increases in intensity when up-chirping the laser pulse. This effect is especially visible in Fig. 3, e.g., compare the spectrum at -280 fs^2 with $+840$ fs^2. In Sec. IV B 2, we will discuss a possible interpretation of the up-chirping control mechanism.

B. Mechanism of chirped multiphoton control

1. Previous chirp experiments using LIF or TOF-mass detection

The effect of chirped femtosecond laser pulses in multiphoton excitation was early on studied in molecules such as Na_2,[45] I_2,[30] and CH_2I_2,[31] and recently in systems such as N_2 (Ref. 46) and polyatomic fragmentation.[11,47]

In the experiments on the multiphoton chirped enhancement of fluorescence in I_2, various mechanisms were discussed such as time-delay resonance, wavepacket following, and sequential resonance.[30] Very recently, Whitaker and co-workers[48] reported a more extensive experimental and theoretical study on the enhancement of three-photon absorption in I_2 and conclude that in this system the observed control is due to time-delay resonance in the second step of the three-photon excitation.

Dantus and co-workers[31] studied the concerted elimination of molecular I_2 from the multiphoton excitation of CH_2I_2. The molecular dissociation product was detected by fluorescence from electronically excited $I_2(D')$. Under irradiation with femtosecond pulses centered near 624 nm the maximum fluorescence yield was found for negatively chirped pulsed around -500 fs^2 and minimum fluorescence was observed at positively chirped pulses of 2400 fs^2 with a factor of 2.9 change in the fluorescence yield. Multiphoton excitation at 312 nm resulted in the opposite effect with the minimum yield found at -500 fs^2 and the maximum at about 2400 fs^2 with enhancements up to 25 for positive chirps. To the best of our knowledge no physical interpretation of the mechanism of the chirp effect was reported to date.

The group of Dantus and co-workers[11] has reported on a very extensive study of strong field fragmentation dynamics with shaped femtosecond laser pulses in some 16 different polyatomic molecules. They conclude that in all these systems there is basically no coherent mechanism involved in the fragmentation but largely an enhanced fragmentation with chirped pulses due to additional absorption of photons by the parent ion. The sign of the chirp played no role in these experiments. However, in a very recent experiment by Goswani *et al.*[47] a very specific chirp effect was reported for the $C_3H_3^+$ and $C_5H_5^+$ fragments produced in the strong-field induced fragmentation in n-propyl benzene. Also for these results no physical mechanism was reported to explain these results.

Weinacht and co-workers[32–34] have recently reported several papers on the strong-field wave-packet driven dissociation and concerted elimination in CH_2I_2 and ionic fragmentation in CH_2BrI and CH_2ClI. These experiments were carried out with 800 nm pulses with pulse intensities of $1-2\times10^{14}$ Watt/cm^2. From these experiments and calculations they conclude that the fragmentation mechanism in pump-probe excitation is due to resonances in the ionic potentials, especially between the ground state of the parent ion and the third electronically excited dissociative parent ion. All the experiments were performed with TOF-ion detection providing no information beyond the mass of the detected species such as, e.g., the kinetic energy of fragmentation products or the angular recoil distribution of fragment ions.

The control of CH_2BrCl ionic fragmentation channels was studied in 2002 by Gerber and co-workers[28] using 800 nm shaped laser pulses in a feedback controlled liquid-crystal-display (LCD) pulse shaper. With transform limited laser pulses of 80 fs duration and energy of 240 μJ/pulse they observed a fragment ratio $CH_2Br^+/CH_2Cl^+ \approx 7\%$ [Fig. 1a in Ref. 28]. With feedback controlled laser pulses they were able to increase this fragment ratio to about 12% (Fig. 2 in Ref. 28). In these strong field experiments at 800 nm, almost zero parent CH_2BrCl^+ ions were observed. Interestingly, when Gerber and co-workers used 400 nm excitation with transform-limited laser pulses of about 5 μJ/pulse they observed a significant parent CH_2BrCl^+ ion signal with a CH_2Cl^+/CH_2BrCl^+ ratio of about 2.3. This is quite similar to the ratio of about 3.1 that we observe in the present experiments at 509 nm. These large changes in the mass spectrum with wavelength observed by Gerber and co-workers[28] suggest that probably a quite different mechanism is responsible for ion fragmentation in strong field ionization at 800 nm versus multiphoton excitation at 400 nm. Interestingly, the optimal pulse shape of the 800 nm pulse that is found to enhance the CH_2Br^+/CH_2Cl^+ ratio resembles a down-chirped pulse (see Fig. 3 in Ref. 28). Although the authors speculate about a possible mechanism for the control mechanism of the pulse shaping results at 800 nm[28] and question whether parent ion surfaces are involved or perhaps highly excited ion-pair states of the neutral they cannot offer any more insight on the mechanism based on the ion masses only.

Theoretical studies on quantum control with shaped laser pulses in CH_2BrCl were performed by Gonzalez and co-workers.[49–53] Extensive electronic structure and dynamics calculations were performed to study the photochemistry of CH_2BrCl and the role of conical intersections between the $\tilde{A}(b\ ^1A')$ and $\tilde{B}(c\ ^1A')$ repulsive surfaces, located with minima near 6.12 and 7.18 eV, respectively.

2. Elucidating control mechanism with photoelectron and ion imaging

As discussed above in Sec. IV A, the CH_2BrCl^+ parent ion and the $CH_2Cl^+ + Br$ fragmentation channel are both produced in a five-photon excitation process. We assign the two

photoelectron peaks separated by some 0.3–0.4 eV (Figs. 3–5) to originate from excitation of the $n_y(Br,8a'')$ and $n_x(Br,22a')$ CH_2BrCl molecular lone-pair orbitals located at the Br-atom.[43,44,49] We use the molecular frame convention of Gonzalez and co-workers[49] labeling the Br–C–Cl plane as the *xz*-plane and the *y*-axis perpendicular to the molecular C_s plane.

From our photoelectron images, we find that the two photoelectron peaks have different laboratory frame angular distributions, $I(\theta) \propto (1+\beta_{2,e}P_2(\cos\theta))$, which also appear to change somewhat with excitation wavelength. At 540 nm excitation, we find for the two photoelectron peaks (see Fig. 4) and short pulses (0 fs^2), $\beta_{2,e}(8a'';0.25\ eV) \approx 0.22$ and $\beta_{2,e}(22a';0.65\ eV) \approx 0.9$. For excitation at higher energy with pulses centered at 509 nm and short pulses (0 fs^2) we find (see Fig. 5), $\beta_{2,e}(8a'';1.10\ eV) \approx 0.62$ and $\beta_{2,e}(22a';1.40\ eV) \approx 0.9$. For the chirped data at 521 nm excitation (see Fig. 3) the two photoelectron peaks at up-chirped pulses (+840 fs^2) have angular distributions characterized by $\beta_{2,e}(8a'';0.87\ eV) \approx 0.62$ and $\beta_{2,e}(22a';1.25\ eV) \approx 1.15$.

The photoelectron peak at low energy that is observed at 521 and 509 nm (but not at 540 nm), and is assigned to five-photon excitation with subsequent fragmentation to $CH_2Cl^+ + Br$ (see Sec. IV A), has a much lower angular anisotropy. At 521 nm and positive up-chirped pulses (+840 fs^2 in Fig. 3), we find $\beta_{2,e}(CH_2Cl^+;0.18\ eV) \approx 0.3$ and at 509 nm excitation and short pulses (0 fs^2 in Fig. 5) $\beta_{2,e}(CH_2Cl^+;0.3\ eV) \approx 0.4$.

The highest energy photoelectron peak (22a′) grows in at positive chirp relative to the intensity of the lower photoelectron peak (8a″), especially well visible for excitation at 521 nm (Fig. 3). So, this excitation of the symmetric in plane $n_x(Br,22a')$ CH_2BrCl molecular lone-pair orbital is enhanced by up-chirped pulses. And at the same time the up-chirp also enhances the photolectron peak at very low energy near 0.18 eV associated with the five-photon fragmentation channel $CH_2Cl^+ + Br(^2P_{3/2})$.

The ion images of the fragmentation channel $CH_2Cl^+ + Br(^2P_{3/2})$ show that the total kinetic energy is very low (Fig. 6) and peaks around 0.05 to 0.08 eV with a FWHM going out to a maximum kinetic energy of about 0.2 eV. The analysis of the angular distribution of the images of the CH_2Cl^+ recoil around the most probable kinetic energy shows that there is no anisotropy, $\beta_{2,CH_2Cl^+} \approx 0$. Both these observations suggest that the formation of this fragmentation channel, after releasing a characteristic low energy photoelectron, is rather statistical. The fragmentation to CH_2Cl^+ is not produced on a very repulsive part of the potential energy surface as that normally leads to high kinetic energy fragments with an anisotropic angular distribution.

The ground state electronic surface of CH_2BrCl^+ has A′ symmetry, and correlates to the lowest fragmentation channel $CH_2Cl^+ + Br(^2P_{3/2})$. The total energy of 11.9 eV after five-photon excitation at 521 nm and the ejection of a 0.1–0.2 eV electron brings the system at an energy of 11.7–11.8 eV just above the energetic threshold of 11.509 eV, but below the energy threshold of 11.966 eV of the spin-orbit excited $CH_2Cl^+ + Br(^2P_{1/2})$ channel.

Up-chirped pulses at 521 nm enhance the $CH_2Cl^+ + Br(^2P_{3/2})$ fragmentation channel, and favor the ejection of the in plane $n_x(Br,22a')$ electron orbital relative to the antisymmetric $n_y(Br,8a'')$ electron orbital. So the question is: why do up-chirped pulses provide a mechanism to enhance the excitation of this orbital in conjunction with enhanced fragmentation?

Because we are dealing with a five-photon excitation and the mechanism is clearly enhanced in only a rather narrow wavelength region we want to discuss the location of several intermediate potential energy surfaces that may play a role in the mechanism. Ng and co-workers[54] have reported the most recent detailed study of the photodissociation dynamics of neutral CH_2BrCl in the wavelength region of 193–267 nm. It is to be noticed here that a two-photon excitation at 521 nm is energetically the same as one-photon excitation in the red-part (261 nm) of the study of Ng and co-workers. The photodissociation around 260 nm mainly produces $CH_2Cl + Br(^2P_{3/2})$ (about 90%), i.e., it predominantly leads to the formation of ground state $Br(^2P_{3/2})$, and only about 10% of spin-orbit excited $Br(^2P_{1/2})$. Furthermore, the photodissociation of the $CH_2Cl + Br(^2P_{3/2})$ channel results in a bimodal (slow, fast) translational energy distribution which they assign to contributions from the [2A′,1A″] and 3A′ surfaces for the slow and fast channel, respectively. The slow channel dominates with a contribution of about 60% versus the fast channel with a contribution of about 40% near 260 nm excitation. Furthermore, at this wavelength the available excitation in the slow channel is for about 65% funneled into internal energy of the neutral CH_2Cl fragment, and from impulsive model calculations[54] they estimate this energy to be split to 10% in rotational energy and 55% vibrational energy. They expect that the vibrational energy is mostly funneled in out-of-plane vibrations of CH_2Cl.

High-level *ab initio* calculations by Gonzalez and co-workers[49] provide information on the principal configuration of the various lowest valence and Rydberg states of CH_2BrCl. The lowest electronically excited valence states result from the $n_x(Br) \rightarrow \sigma^*(C-Br)(2A')$ and $n_y(Br) \rightarrow \sigma^*(C-Br)(1A'')$ excitations. The lowest states of Rydberg character, $n_x(Br) \rightarrow Rydberg(A')$ and $n_y(Br) \rightarrow Rydberg(A')$, are located near 7.4 eV. This is very close to three-photon excitation of 521 nm (7.2 eV). These A′,A″ Rydberg states have by far the largest oscillator strength in an one-photon excitation of all the excitations up to about 9 eV (see Table III in Ref. 49).

Considering our experimental results and the discussion above, we therefore propose that the up-chirp enhancement of the ejection of the in plane $n_x(Br,22a')$ electron orbital in the five-photon process is a manifestation of either wave-packet following or a time-delay resonance between the dissociative (2A′) surface, reached via two-photon excitation, and the Rydberg (A′) surface located at three-photon excitation. Because the (2A′) surface is strongly repulsive in the C–Br coordinate an up-chirped pulse will provide a more enhanced coupling with the higher-lying $n_x(Br)$ Rydberg (A′) state. The Rydberg (A′) state serves as the stepping stone for further two-photon excitation into the $CH_2BrCl^+(\tilde{X}\ A')$ continuum. In the whole five-photon exci-

tation process it is the $n_x(Br,22a')$ electron orbital that appears to be enhanced more by the up-chirp relative to the $n_y(Br,8a'')$ electron. Furthermore, the dynamics on the $(2A')$ repulsive surface after two-photon excitation may also lead to a more favorable geometric configuration of the CH_2BrCl molecule such that subsequent excitation via the Rydberg (A') state to the five-photon excited CH_2BrCl molecule leads to a specific electron channel near low energy (0.1–0.2 eV) and the formation of the $CH_2Cl^+ + Br(^2P_{3/2})$ fragmentation channel just above threshold. A schematic of the proposed mechanism is shown in Fig. 7.

It would be highly desirable to have more theoretical calculations on the two-photon excited wavepacket dynamics on the dissociative $(2A')$ surface and subsequent excitation by a third chirped-photon to a higher lying state, possible the lowest Rydberg (A') state.

V. CONCLUSIONS

In this paper we have reported on first experiments combining velocity map photoelectron and ion imaging detection with chirped pulse excitation to control the photoionization and fragmentation in CH_2BrCl. The experiments show that there is a limited spectral window near 521 nm where up-chirped pulses can strongly increase the CH_2Cl^+/CH_2BrCl^+ ion ratio by almost five times. The photoelectron images and the CH_2Cl^+ ion image give conclusive information that both the photoionization and the fragmentation are induced by a five-photon excitation. The photoelectron peaks at higher energy can be assigned to the ionization of the $n_x(Br,22a')$ and $n_y(Br,8a'')$ electron orbitals. The up-chirp favors the ejection of the symmetric $n_x(Br,22a')$ orbital which leads to formation of the symmetric $CH_2BrCl^+(\tilde{X}\ A')$ ground state of the parent ion. Furthermore, the enhanced fragmentation at 521 nm also leads to the formation of an extra photoelectron peak near 0.1–0.2 eV that is correlated with the $CH_2Cl^+ + Br(^2P_{3/2})$ fragmentation channel just above threshold. We propose that a wavepacket following or time-delay resonance between the dissociative two-photon excited $(2A')$ state and the three-photon resonant Rydberg (A') state is responsible for the enhanced excitation of the $n_x(Br,22a')$ orbital through these higher lying near-resonances. The intermediate dynamics on the dissociative two-photon excited $(2A')$ surface leads to a geometrical deformation of the CH_2BrCl molecule such that the subsequent ionization at the five-photon level explores a part of the multi-dimensional ion-continuum of the $CH_2BrCl^+(\tilde{X}\ A')$ ground state above the dissociation limit of the $CH_2Cl^+ + Br(^2P_{3/2})$ fragmentation channel. This leads to an enhanced fragmentation with near statistical (low) kinetic energy of the fragments and an isotropic angular distribution. At present we are performing full photoelectron-photoion coincidence experiments of CH_2BrCl in our newly developed apparatus in Amsterdam[26,27,55] with full adaptive LCD-pulse shaping. We hope that such more advanced coincidence experiments will provide additional information that in combination with theoretical dynamics calculations will reveal the definite mechanism of the pulse shaping control in the multiphoton photodynamics of CH_2BrCl.

ACKNOWLEDGMENTS

This research has been financially supported by the council for Chemical Sciences of the Dutch Organization for Scientific Research (NWO-CW). The authors also acknowledge support by the European Union through the Integrated Infrastructure Initiative LaserLabEurope and the Marie-Curie Initial Training Network ICONIC. The authors gratefully acknowledge discussions with Professor L. Gonzalez (Jena), Professor T. Rozgonyi (Budapest), and Dr. V.P. Nicu (Amsterdam) on electronic structure calculations of CH_2BrCl.

[1] D. J. Tannor and S. A. Rice, J. Chem. Phys. **83**, 5013 (1985).
[2] P. Brumer and M. Shapiro, Chem. Phys. Lett. **126**, 541 (1986).
[3] R. S. Judson and H. Rabitz, Phys. Rev. Lett. **68**, 1500 (1992).
[4] J. L. Herek, J. Photochem. Photobiol., A **180**, 225 (2006).
[5] H. Fielding, M. Shapiro, and T. Baumert, J. Phys. B **41**, 070201 (2008).
[6] H. Rabitz, New J. Phys. **11**, 105030 (2009).
[7] A. Assion, T. Baumert, M. Bergt, T. Brixner, B. Kiefer, V. Seyfried, M. Strehle, and G. Gerber, Science **282**, 919 (1998).
[8] R. J. Levis, G. M. Menkir, and H. Rabitz, Science **292**, 709 (2001).
[9] X. Zhu, T. C. Gunaratne, V. V. Lozovoy, and M. Dantus, J. Phys. Chem. A **113**, 5264 (2009).
[10] R. J. Levis, J. Phys. Chem. A **113**, 5267 (2009).
[11] V. V. Lozovoy, X. Zhu, T. C. Gunaratne, D. A. Harris, J. C. Shane, and M. Dantus, J. Phys. Chem. A **112**, 3789 (2008).
[12] C. Daniel, J. Full, L. Gonzalez, C. Lupulescu, J. Manz, A. Merli, S. Vajda, and L. Woste, Science **299**, 536 (2003).
[13] D. W. Chandler and P. L. Houston, J. Chem. Phys. **87**, 1445 (1987).
[14] D. W. Chandler, J. W. Thoman, Jr., M. H. M. Janssen, and D. H. Parker, Chem. Phys. Lett. **156**, 151 (1989).
[15] M. H. M. Janssen, D. H. Parker, G. O. Sitz, S. Stolte, and D. W. Chandler, J. Phys. Chem. **95**, 8007 (1991).
[16] M. H. M. Janssen, J. W. G. Mastenbroek, and S. Stolte, J. Phys. Chem. A **101**, 7605 (1997).
[17] T. Suzuki and B. J. Whitaker, Int. Rev. Phys. Chem. **20**, 313 (2001).
[18] A. Stolow, Annu. Rev. Phys. Chem. **54**, 89 (2003).
[19] T. P. Rakitzis, A. J. van den Brom, and M. H. M. Janssen, Science **303**, 1852 (2004).
[20] M. N. R. Ashfold, N. H. Nahler, A. J. Orr-Ewing, O. P. J. Vieuxmaire, R. L. Toomes, T. N. Kitsopoulos, I. A. Garcia, D. A. Chestakov, S.-M. Wu, and D. H. Parker, Phys. Chem. Chem. Phys. **8**, 26 (2006).
[21] O. Gessner, A. M. D. Lee, J. P. Shaffer, S. V. Reisler, S. V. Levchenko, A. I. Krylov, J. G. Underwood, H. Shi, A. L. L. East, D. M. Wardlaw, E. T. Chrysostom, C. C. Hayden, and A. Stolow, Science **311**, 219 (2006).
[22] T. Suzuki, Annu. Rev. Phys. Chem. **57**, 555 (2006).
[23] A. I. Chichinin, K.-H. Gericke, S. Kauczok, and C. Maul, Int. Rev. Phys. Chem. **28**, 607 (2009).
[24] J. A. Davies, J. E. LeClaire, R. E. Continetti, and C. C. Hayden, J. Chem. Phys. **111**, 1 (1999).
[25] A. M. Rijs, M. H. M. Janssen, E. T. H. Chrysostom, and C. C. Hayden, Phys. Rev. Lett. **92**, 123002 (2004).
[26] A. Vredenborg, W. G. Roeterdink, and M. H. M. Janssen, J. Chem. Phys. **128**, 204311 (2008).
[27] A. Vredenborg, W. G. Roeterdink, and M. H. M. Janssen, Rev. Sci. Instrum. **79**, 063108 (2008).
[28] N. H. Damrauer, C. Dietl, G. Krampert, S. H. Lee, K. H. Jung, and G. Gerber, Eur. Phys. J. D **20**, 71 (2002).
[29] B. Amstrup, J. D. Doll, R. A. Sauerbrey, G. Szabo, and A. Lorincz, Phys. Rev. A **48**, 3830 (1993).
[30] V. V. Yakovlev, C. J. Bardeen, J. Che, J. Cao, and K. R. Wilson, J. Chem. Phys. **108**, 2309 (1998).
[31] I. Pastirk, E. J. Brown, Q. Zhang, and M. Dantus, J. Chem. Phys. **108**, 4375 (1998).
[32] D. Geißler, B. J. Pearson, and T. Weinacht, J. Chem. Phys. **127**, 204305 (2007).
[33] B. J. Pearson, S. R. Nichols, and T. Weinacht, J. Chem. Phys. **127**, 131101 (2007).
[34] S. R. Nichols, T. C. Weinacht, T. Rozgonyi, and B. J. Pearson, Phys. Rev. A **79**, 043407 (2009).
[35] W. G. Roeterdink and M. H. M. Janssen, Chem. Phys. Lett. **345**, 72 (2001).

[36] W. G. Roeterdink and M. H. M. Janssen, Phys. Chem. Chem. Phys. **4**, 601 (2002).
[37] D. Irimia, R. Kortekaas, and M. H. M. Janssen, Phys. Chem. Chem. Phys. **11**, 3958 (2009).
[38] D. Irimia, I. D. Petsalakis, G. Theodorakopoulos, and M. H. M. Janssen, J. Phys. Chem. A **114**, 3157 (2010).
[39] M. L. Lipciuc and M. H. M. Janssen, Phys. Chem. Chem. Phys. **8**, 3007 (2006).
[40] T. Wilhelm, J. Piel, and E. Riedle, Opt. Lett. **22**, 1494 (1997).
[41] G. Cerullo and S. De Silvestri, Rev. Sci. Instrum. **74**, 1 (2003).
[42] I. Z. Kozma, P. Baum, U. Schmidhammer, S. Lochbrunner, and E. Riedle, Rev. Sci. Instrum. **75**, 2323 (2004).
[43] S. X. Tian, N. Kishimoto, and K. Ohno, J. Phys. Chem. A **107**, 2137 (2003).
[44] J. Li, J. Yang, Y. Mo, K. C. Lau, X. M. Qian, Y. Song, J. Liu, and C. Y. Ng, J. Chem. Phys. **126**, 184304 (2007).
[45] A. Assion, T. Baumert, J. Helbing, V. Seyfried, and G. Gerber, Chem. Phys. Lett. **259**, 488 (1996).
[46] J. Plenge, A. Wirsing, C. Raschpichler, M. Meyer, and E. Ruhl, J. Chem. Phys. **130**, 244313 (2009).
[47] T. Goswami, S. K. K. Kumar, A. Dutta, and D. Goswami, Chem. Phys. **360**, 47 (2009).
[48] N. T. Form, B. J. Whitaker, and C. Meier, J. Phys. B **41**, 074011 (2008).
[49] T. Rozgonyi, T. Feurer, and L. Gonzalez, Chem. Phys. Lett. **350**, 155 (2001).
[50] T. Rozgonyi and L. Gonzalez, J. Phys. Chem. A **106**, 11150 (2002).
[51] T. Rozgonyi and L. Gonzalez, J. Phys. Chem. A **110**, 10251 (2006).
[52] T. Rozgonyi and L. Gonzalez, J. Phys. Chem. A **112**, 5573 (2008).
[53] T. Rozgonyi and L. Gonzalez, J. Mod. Opt. **56**, 790 (2009).
[54] J. Zhou, K.-C. Lau, E. Hassanein, H. Xu, S.-X. Tian, B. Jones, and C. Y. Ng, J. Chem. Phys. **124**, 034309 (2006).
[55] A. Vredenborg, W. G. Roeterdink, and M. H. M. Janssen, Chem. Phys. Lett. **478**, 20 (2009).